MARTIAN THERMOSPHERE IN MAVEN/IUVS DATA AND MPI-MGCM.

C. Mockel, A. S. Medvedev, P. Hartogh, *Max Planck Institute for Solar System Research, Göttingen, Germany (mockel@mps.mpg.de)*, **E. Yiğit,** *George Mason University, Fairfax, USA*, **H. Nakagawa, N. Terada, T. Kuroda,** *Department of Geophysics, Tohoku University, Sendai, Japan*, **K. Seki,** *Department of Earth and Planetary Science, University of Tokyo, Tokyo, Japan*, **S. Evans,** *Computational Physics, Inc., Springfield, Virginia, USA*, **N. M. Schneider, S. K. Jain, J. I. Deighan, W. E. McClintock, B. M. Jakosky,** *Laboratory for Atmospheric and Space Physics, University of Colorado Boulder, Boulder, Colorado, USA*, **D. Lo,** *Lunar and Planetary Laboratory, University of Arizona, Tucson, Arizona, USA*.

Introduction

The Imaging Ultraviolet Spectrograph as part of the MAVEN orbiter (MAVEN/IUVS) measures airglow emissions, which allows for retrieving major atmospheric species. In addition to CO_2, MAVEN/IUVS provides profiles of atomic oxygen. We compare simulations with the Max Planck Institute Martian Global Circulation Model (MPI-MGCM, or MAOAM) [Hartogh et al., 2005] with MAVEN/IUVS data. This comparison provides insights into the physical and dynamical processes in the Martian thermosphere that maintain the circulation and day-to-day variability. In an early comparison [Medvedev et al.,2015], we highlighted various combinations that can explain the conditions as observed by the spacecraft. With more observational data, in particular on atomic oxygen abundances, we constrain these processes further to improve the predictive capabilities of the MGCM.

Thermosphere

Four major processes listed below affect the circulation in the Martian thermosphere.

- Atomic oxygen abundances through facilitation of the cooling due to radiative transfer in the 15μm band of CO_2 molecules;
- Absorption of the solar EUV radiation is the main source of energy in the thermosphere. Fluctuations of the solar EUV flux directly affect temperature in the thermosphere;
- Aerosols in the Martian lower and middle atmosphere absorb IR radiation and modulate the underlying circulations. These dust-induced changes can reach thermospheric heights [Medvedev et al.,2013];
- Gravity waves transport momentum and energy across atmospheric layers and deposit them in the thermosphere upon dissipation and breaking [Yiğit and Medvedev, 2015]

The simulations have been focused on constraining these processes through a comparison with the MAVEN/IUVS retrievals.

Retrievals

MAVEN/IUVS measures the mid and far-UV airglow. Number densities (level 2, version 4) of four major atmospheric constituents (CO_2, N_2, O, CO^+) have been retrieved using a forward model [Evans et al., 2015]. The one Earth year of observations cover all longitudes, and sample the low and mid latitudes. The data comprises observations from the northern hemisphere fall to summer (solar longitude L_s from 210° to 70°). The measurements depend on the solar zenith angle and, thus, are limited by local time from 08 to 15 hr.

Atomic oxygen

The retrieved atomic oxygen follows a seasonal cycle similar to the other constituents, but does not show a well-defined longitudinal or latitudinal structure. The retrieved highly variable number densities [O] have been converted into the volume mixing ratios and averaged into a global mean vertical profile (labeled as the “IUVS scenario"). This allows for a direct comparison with the oxygen scenarios based on photochemical models (the Nair model, N94 [Nair et al., 1994], and Mars Climate Database, MCD [González-Galindo et al., 2009]) presented in Figure 1.

The period prior to apoapsis was chosen for the comparing the atmospheric response to the choice of oxygen scenario because of the moderate solar activity and absence of dust storms. As seen in Figure 2, the simulation with the largest [O] volume mixing ratio (MCD scenario) results in the lowest simulated CO_2 number density. The effect is noticeable above $\sim$120 km and is negligible below. The reduced oxygen abundance for the other two simulations yields better agreement between the simulations and IUVS observations. The large variation (illustrated by the bars), however, reduce the robustness of this conclusion. Temperature follows the similar trend, with the N94 scenario resulting in the

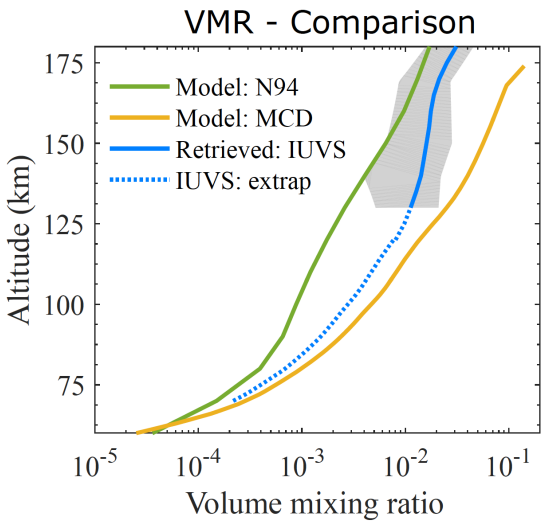

Figure 1: Comparison of 1-D volume mixing profiles, grey area indicates 1 standard deviation. The MAVEN/IUVS retrieval is given by the blue line, green and yellow distinguish between the two photochemical modeling profiles.

warmest simulated atmosphere, the MCD run producing the coldest atmosphere, and the IUVS scenario falling between the two.

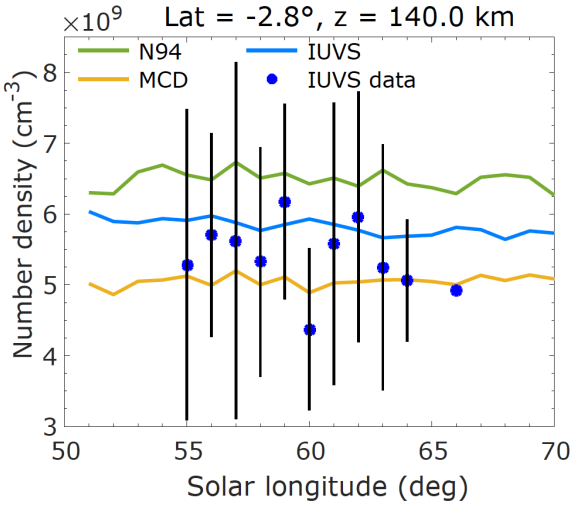

Figure 2: Effect of the different atomic oxygen volume mixing ratios on the zonally averaged CO_2 number density for the indicated latitude and altitude. Blue dots show the zonally averaged MAVEN/IUVS retrievals, bars indicate 1 standard deviation.

EUV flux

Simulations have been performed to test the atmospheric response do daily variations of the $F_{10.7}$ flux, a proxy for the EUV activity of the Sun. At the end of the Martian year, the observations sampled nearly a full 27-day solar cycle, which allowed us to test its impact on the thermosphere. The atmospheric temperature response was instantaneous, with the strongest effect being at high altitudes and exponentially decaying below. Figure 3 displays the temperature variations for the three different oxygen profiles, compared to a baseline scenario of constant solar flux $F_{10.7}$. The strength of the impact depends on the atomic oxygen scenario. The N94 scenario shows the largest temperature fluctuations. The agreement with the observations increases during the first phase of the cycle, and decreases during the second part of the cycle. The simulated CO_2 number density is less sensitive to the EUV flux. Overall, the N94 simulations also produce the largest simulated number density in agreement with the observations.

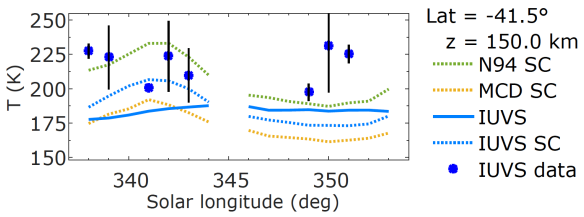

Figure 3: The impact of changes in the solar intensity on the zonally averaged CO_2 number density. Dashed lines indicate simulations with the 27-day solar cycle included. The effect was tested for all three different oxygen scenarios. Blue dots present the zonally averaged MAVEN/IUVS retrievals, bars indicate 1 standard deviation.

Dust activity

Dust activity typically increases in the second half of the Martian year. Around $L_s \sim 320°$, the dust opacity has been obtained through concurrent observations of Mars Climate Sounder (MCS) onboard the Mars Reconnaissance Orbiter (MRO) [Kleinböhl et al., 2009] and input into the model. Thus simulated CO_2 number density is in a better agreement with the MAVEN/IUVS retrievals than in the reference run with a constant dust load, (see Figure 4). Temperatures above the homopause show little sensitivity to variations of dust opacity.

All the presented simulations have been performed accounted for parameterized effects of subgrid-scale gravity waves. Without gravity waves (NGW), the the agreement between the simulations and observations deteriorates.

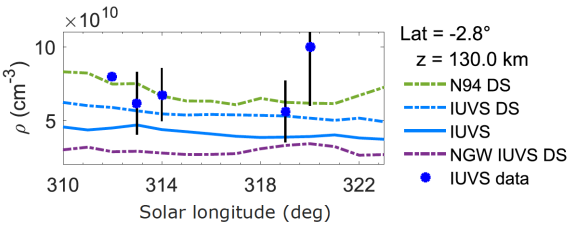

Figure 4: Effect of changes in the dust opacity on the zonally averaged CO_2 number density for the indicated latitude and altitude. Dashed-dotted lines are for runs including the MRO/MCS dust opacity, the solid line is for the reference simulation. Blue dots present the zonally averaged MAVEN/IUVS retrievals, bars indicate 1 standard deviation.

References

Evans, J. S., et al. (2015), Retrieval of CO2 and N2 in the Martian thermosphere using dayglow observations by IUVS on MAVEN, Geophys. Res. Lett., 42.

González-Galindo, F. ,et al., (2009), A ground-to-exosphere Martian general circulation model: 1. Seasonal, diurnal, and solar cycle variation of thermospheric temperatures, J. Geophys. Res., 114.

Hartogh, P., et al., (2005), Description and climatology of a new general circulation model of the Martian atmosphere, J. Geophys. Res., 110.

Kleinböhl, A., et al., (2009), Mars Climate Sounder limb profile retrieval of atmospheric temperature, pressure, and dust and water ice opacity, J. Geophys. Res. Planets, 114.

Nair, H., et al., (1994), A photochemical model of the Martian atmosphere, Icarus, 111, 124-150.

Medvedev, A. S., E. Yiğit, T. Kuroda, and P. Hartogh (2013), General circulation modeling of the Martian upper atmosphere during global dust storms, J. Geophys. Res. Planets, 118, 22342246, doi:10.1002/2013JE004429.

Medvedev, A. S., et al. (2015), Comparison of the Martian thermospheric density and temperature from IUVS/MAVEN data and general circulation modeling, Geophys. Res. Lett., 43.

Yiğit, E., and A. S. Medvedev (2015), Internal wave coupling processes in Earthâ^s atmosphere, Adv. Space Res., 55, 983-1003, doi:10.1016/j.asr.2014.11.020.